

Original Article

Comparison of tissue changes caused by microwave and radio frequency energy in an experimental liver ablation

Nguyen Quoc Vinh^{1,2}, Tohru Tani³, Shigeyuki Naka^{1,3}, Soichiro Tani^{1,3}

¹Department of Surgery, Shiga University of Medical Science, Seta-Tsukinowa, Otsu City, Shiga 520-2192, Japan; ²Department of General Surgery, University of Medicine and Pharmacy, Ho Chi Minh City, 217 Hong Bang District 5, Ho Chi Minh City, Vietnam; ³Biomedical Innovation Center, Shiga University of Medical Science, Seta-Tsukinowa, Otsu City, Shiga 520-2192, Japan

Received November 11, 2015; Accepted January 12, 2016; Epub February 1, 2016; Published February 15, 2016

Abstract: Both radiofrequency ablation (RFA) and microwave ablation (MWA) techniques use high temperatures to ablate tissue but with different mechanisms. An understanding of differences in tissue reactions to these physical mechanisms may provide helpful information for practitioners and technical development. In the present study, we subjected rat liver to RFA and MWA under relatively equivalent conditions including power supply, application duration, needle shape, and ablation maneuver. Comparisons were based on changes in tissue color, injury size, and microscopic tissue changes immediately, 12, 24, and 72 h after ablation. The results revealed that the RFA and MWA induced similar changes in tissue color and injury diameter. However, in the central zone, hepatocyte shapes and nuclei were well maintained at each time point after MWA, whereas cellular disruption occurred soon after RFA. In the outer zone, intraregional cell survival and a more irregular burn edge were observed with RFA. AcP staining was useful for early disclosure of ablated zones and definition of non-viable cells in inner zone. In conclusions, MWA and RFA differed with regard to the central zone and peripheral areas with more regular ablated zone observed in MWA. These findings indicate the superiority of MWA over RFA for creating a more reliable and controllable ablation zone.

Keywords: Radiofrequency ablation, microwave ablation, thermal tissue injury, acid phosphatase staining, liver tumor ablation, histological change

Introduction

Over the last few decades, numerous local ablative techniques have been developed for the treatment of non-resectable hepatic tumors, which account for a large proportion of hepatic malignancies. Among these techniques, radiofrequency ablation (RFA) and microwave ablation (MWA) have generated the most interest and have been widely accepted as the techniques of choice for such malignancies [1, 2]. Both techniques incorporate high temperatures to achieve thermal tissue coagulation, but their heating mechanisms are quite different.

RFA uses energy from a radiofrequency current to heat tissue and thus relies on ionic agitation. An alternating electric current at a frequency of

200-1200 kHz passes through the body in a close circuit as a result of the ionic molecules present in tissues. Resistive heating occurs around the electrode according to the Joule effect [3-5]. This heating zone (i.e., direct heating zone) is limited to a millimeter-scale range around the electrode. However, heat conduction enables enlargement of the ablation area. Some technical problems associated with RFA include the increase in tissue impedance during ablation due to water evaporation at temperature of $\geq 100^{\circ}\text{C}$ and tissue charring at temperature of $>200^{\circ}\text{C}$ [6]. In addition, the electric current, which runs in areas of low resistance (i.e., significant ionic component), bypasses areas adjacent to large vessels. This phenomenon results in a heat-sink effect around large vessels.

Comparison of MWA and RFA

MWA relies on a special tissue heating mechanism called dielectric heating, which occurs when an alternating electromagnetic field is applied to an imperfect dielectric material. In microwave-irradiated tissue, water and other polar molecules are forced to oscillate at the applied frequency, a process called dielectric hysteresis. Some of the electromagnetic energy is absorbed and converted to heat [4, 7]. Because microwaves can propagate through non-conductive materials, they are not inhibited by an increase in tissue impedance during ablation, thus allowing a volume of tissue to receive uniform heating [8].

Numerous studies have demonstrated that both ablation methods can induce reliable cell death in the ablation zone and are effective for the treatment of liver tumors [2, 9-11]. Other studies comparing MWA and RFA identified aspects related to clinical applications, such as comparisons of the ablation volume, ablation zone border and shape, technical advantages and disadvantages, and treatment outcomes [4, 12-16]. In these comparisons, the differences between MWA and RFA were a consequent of the specific heating mechanisms. Andreano *et al.* compared tissue heating patterns obtained with microwaves and radiofrequency [17]. However, there is lack of comparative data regarding the tissue effects caused by these heating mechanisms.

In this study, we set up an experimental model in which MWA and RFA were performed under relatively equivalent conditions (e.g., same power output, ablation duration, needle shape, and ablation maneuver) to compare tissue damage and subsequent remodeling processes of ablated regions. Tissue morphology was compared using a conventional hematoxylin and eosin (H&E) staining technique. In addition, acid phosphatase (AcP) staining, an effective method for characterizing early ablation zones, was used to compare alterations in enzymatic activity in the ablated areas.

Materials and methods

Microwave ablation and radiofrequency ablation devices

The MWA system comprises a microwave generator connected to an antenna via a flexible, low-loss coaxial cable. The generator radiates microwave energy from a magnetron (Ma-

gnetron, Alfresa Ltd, Osaka, Japan) at a frequency of 2,450 MHz and can produce power at 1-100 W. The 15-cm 17-gauge needle-shaped antenna includes a coaxial dipole with a 1-cm radiating segment. The RFA device was a Cool-tip™ RF ablation system (Covidien, Boulder, CO, USA), which operates at a 480 KHz, with a controllable output power up to a maximum of 200 W. The RF needle is an internally cooled single electrode (10 cm, 17-gauge, 2 cm exposure). During ablation, chilled saline solution (5°C) was circulated through the needle via a peristaltic pump.

Animal and ablation technique

Experiments were performed under the approval of the Committee on Animal Care. Ten-week-old male Sprague Dawley rats, weighing 280-300 g (CLEA Japan, Inc., Tokyo, Japan), were used for the experiment. Each rat was anesthetized under general anesthesia via isoflurane inhalation. A 3-cm midline incision was made in the upper abdomen to expose the external left lobe of the liver. RFA and MWA were performed using the same maneuvers on the external left lobe of the liver at two sites separated by a 2-cm distance to prevent overlapping injuries. MWA was performed at a power of 20 W and duration of 20 s. RFA was performed using a relatively equivalent amount of energy by maintaining the power at 20 W during 20 s RF activation. Twelve rats in total were received the same MWA and RFA on their external left lobes of the liver. Following each application, the ablated zone was macroscopically evaluated and measured using a Vernier caliper. Each series of three rats was sacrificed immediately and 12, 24, and 72 h after ablation for sample collection. Each ablated lesion was divided equally into two samples; one sample was fixed in 10% formaldehyde and the other was stored at -80°C for subsequent H&E and AcP staining, respectively.

AcP histochemical staining

For AcP histochemical staining, a series of 8- μ m-thick frozen sections were prepared using a cryostat (Leica CM1900, Wetzlar, Germany). We used the diazonium salt coupling method with a naphthol AS series of phosphate esters, as previously described [18]. The incubation solution contained 40 mL of buffer (0.2 M CH₃COOH) with 12 mg of naphthol AS-BI phosphate, 30 mg of Fast red salt, 250 μ l of N,N-

Comparison of MWA and RFA

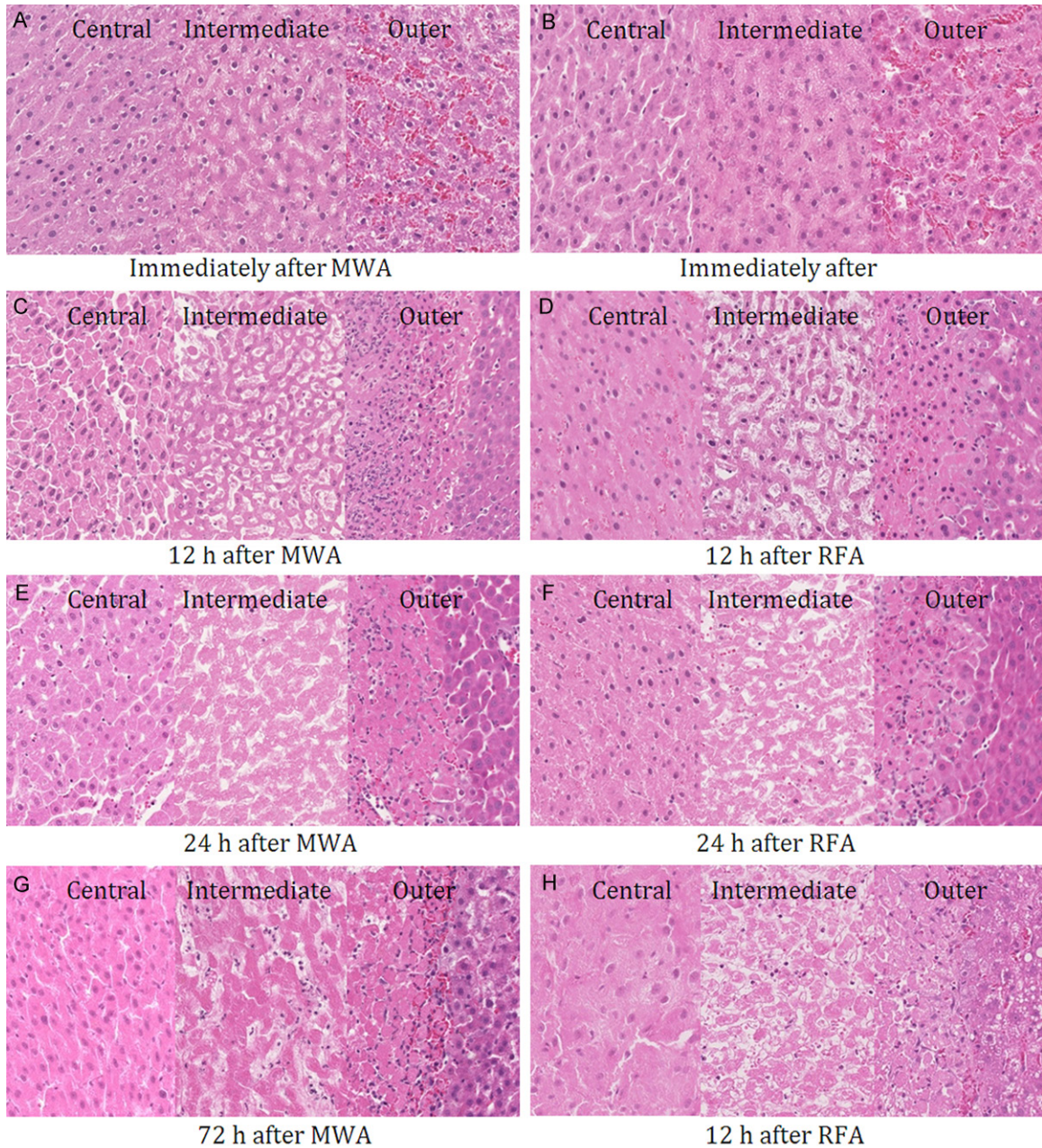


Figure 1. High magnification (400 \times) images of MWA and RFA samples stained with H&E. In the central zone, cells maintained their shapes, membranes, and nuclei at every time point after MWA (A, C, E, and G, left), whereas the cells progressively lost their shapes after RFA (B, D, F, and H, left). In the intermediate zones of both MWA and RFA lesions, swollen hepatocytes with blurred cell walls were invisible immediately after ablation (A, B, middle), tissue edema and nuclear loss were evident later (C-H, middle), and granulocyte and fibroblast infiltration were observed at 72 h after ablation at 72 h after ablation (G-H, middle). In the outer zone, hemorrhage was detected immediately after ablation (A, B, right). Hepatocytes disruption and granulocyte and fibroblast infiltration were observed at later time points (C-H, right)

dimethylformaldehyde, and 2 drops of 10% $MgCl_2$. The sections were incubated in the buffer at 37 $^{\circ}C$ for 30 min. All slice images were captured using a NanoZoomer (2.0-RSC10730-SG, Hamamatsu Photonics, Shizuoka, Japan).

Statistical analysis

The ablated zone diameters were summarized and expressed as mean \pm standard deviations. The means were compared with the indepen-

Comparison of MWA and RFA

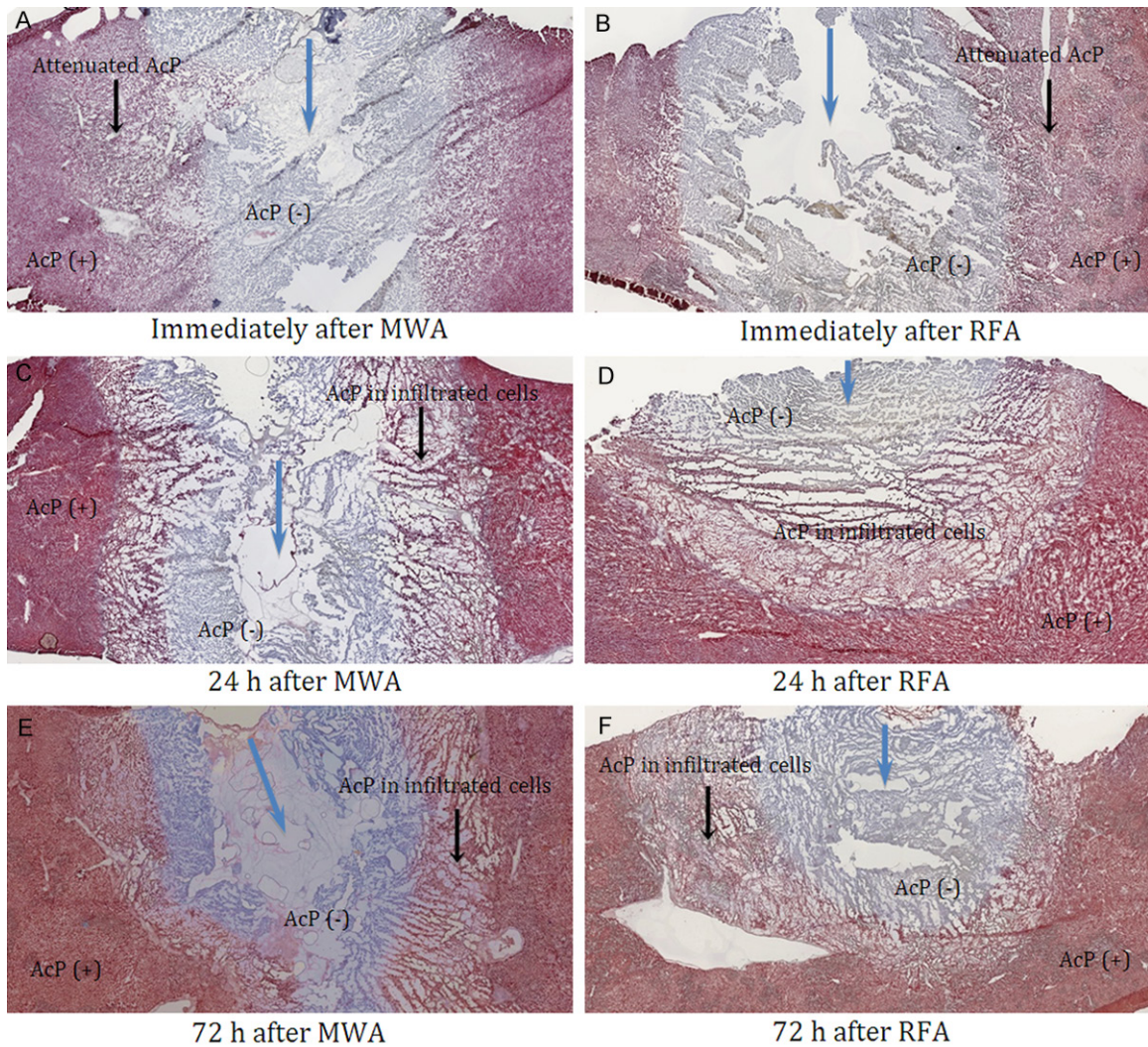


Figure 2. Low magnification (10 \times) images of MWA and RFA samples stained with AcP. Blue arrows indicate the needle insertion sites. AcP activity was absent in the central and intermediate zones. AcP activity was attenuated in the outer zone because of the disappearance of AcP in hepatocytes and concomitant normal AcP activity in the infiltrating cells. No difference in AcP staining was observed between MWA and RFA samples at any time point.

dent sample *t*-test using the SPSS 20.0 statistical software package (SPSS, Inc., Chicago, IL, USA). A *p*-value of <0.05 was considered a statistically significant difference.

Results

All rats tolerated the procedure and no complications were encountered during the experiment. MWA and RFA induced quite similar macroscopic tissue changes. These changes appeared as three contiguous color zones: a brown central zone, pale/white intermediate zone, and purple peripheral rim, which formed a border with the intact liver. The mean surface diameters measured immediately after RFA

and MWA were 6.9 ± 0.3 and 6.7 ± 0.3 mm, respectively. These values were not significantly different ($P = 0.118$). The ablated lesions expanded to average diameters of 9.1 ± 0.2 mm for RFA and 8.8 ± 0.2 mm for MWA at 24 h after ablation ($P = 0.135$).

The comparison of microscopic findings following MWA and RFA was performed immediately and 12, 24, and 72 h after ablation. Immediately after ablation, no differences were observed between the lesions ablated via MWA and RFA with either H&E or AcP staining (**Figures 1A, 1B** and **2A, 2B**). The central zone comprised cells that had maintained their structures but appeared slightly smaller and more eosinophil-

Comparison of MWA and RFA

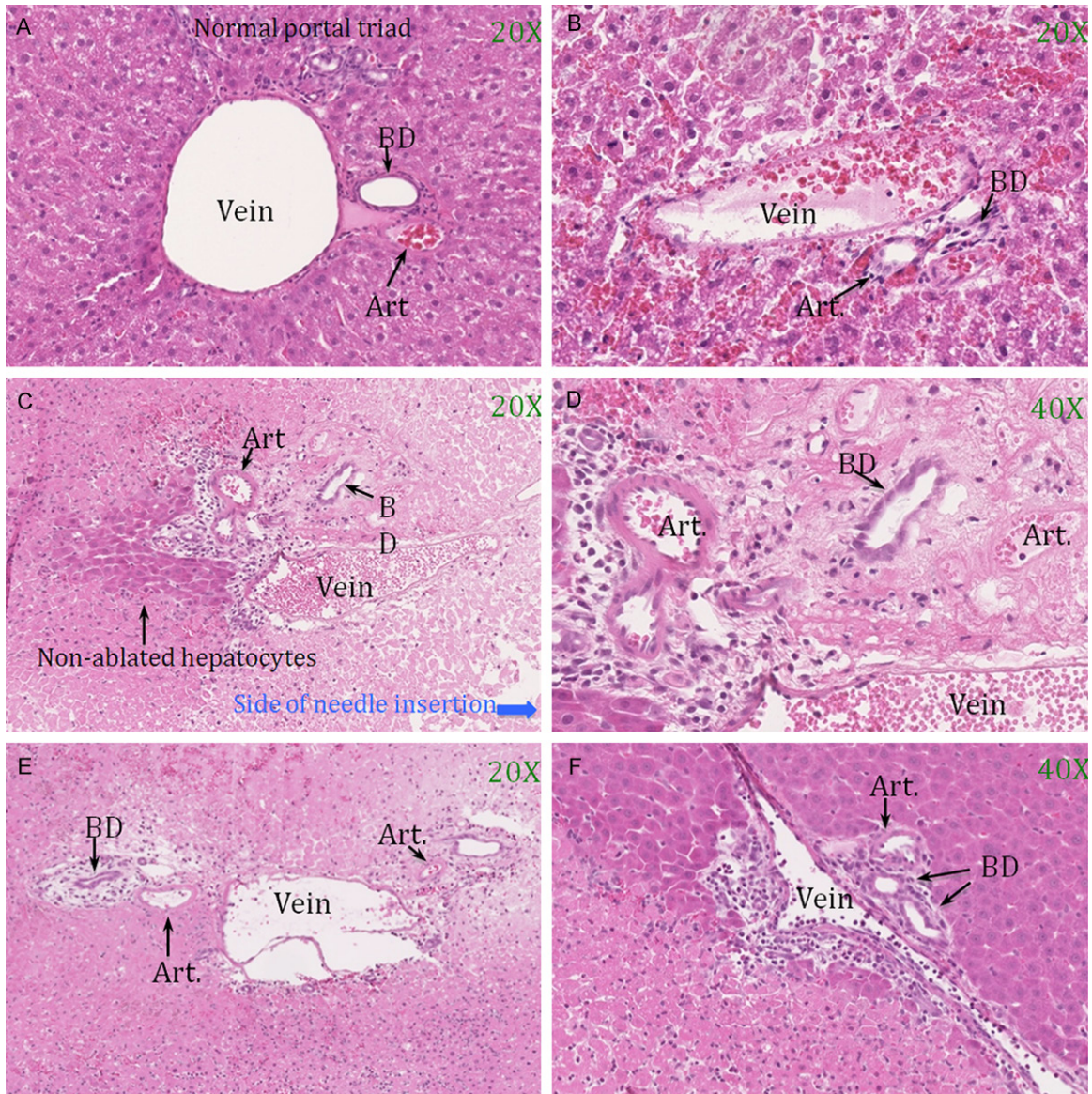


Figure 3. Changes of intrahepatic veins, arteries, and bile ducts in and around ablated regions. A normal hepatic portal triad with portal vein, hepatic artery (Art.), and bile duct (BD) (A). An intra-lesional portal triad at immediately after ablation (B), 24 h after ablation (C and D), and 72 h after ablation (E). A portal triad in neighboring ablated lesion (F).

ic than those in the intact liver (**Figure 1A, 1B**, left). The intermediate zone, which surrounded the central zone, comprised swollen hepatocytes with blurred cell walls and/or nuclear loss (**Figure 1A, 1B**, middle). AcP activity was absent in the central and intermediate zones, indicating that the cells were completely non-viable despite the normal shape of cells in the central zones. The outer zone, corresponding to the purple rim, was characterized by the dilation and congestion of sinusoids with abundant erythrocytes and the presence of intact hepa-

toocytes with distinct cell walls and normal nuclear morphology (**Figure 1A, 1B**, right). AcP activity was slightly attenuated in the outer zone compared with that in the intact liver (**Figure 2A, 2B**).

However, the remodeling processes in the central zones induced by MWA and RFA evolved differently. After MWA, the cells in the central zone maintained their cell shapes, membranes, and nuclei until 72 h after ablation (**Figure 1C, 1E** and **1G**, left). In contrast, cellular disruption

Comparison of MWA and RFA

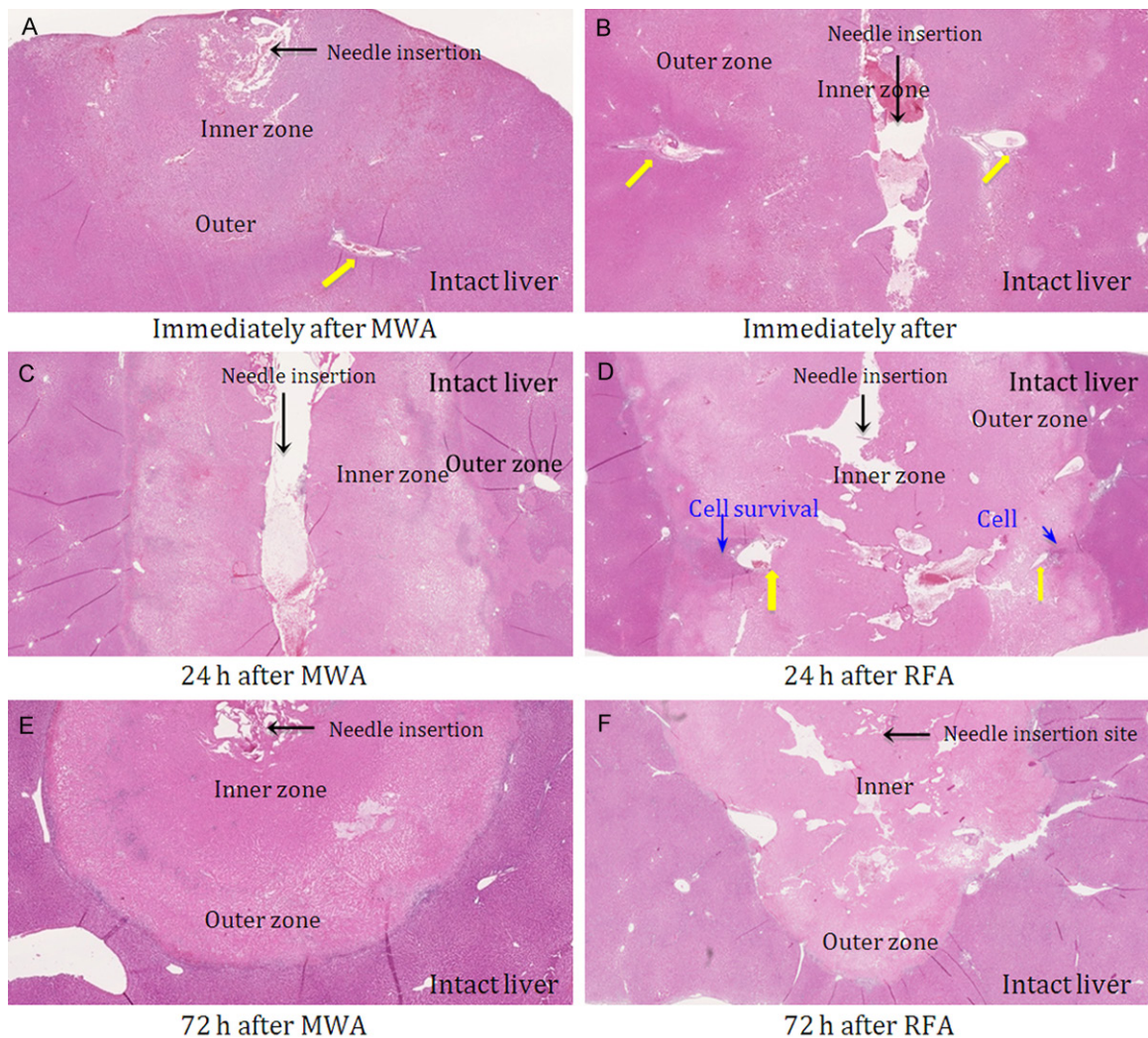


Figure 4. Low magnification (10×) images of MWA and RFA samples stained with H&E. Yellow arrows indicate blood vessels. In RFA, blood vessels caused indentations in the ablation zone (B) and the presence of intralésional cells in outer side of vessel (D). In MWA, the ablation zone was less affected by blood vessels (A) and no intralésional cell survival was observed (C and E). RFA induced a more irregularly shaped ablation zone compared with MWA (E and F).

was evident in some areas of the central zones of RFA samples at 12 h and disruption evolved progressively at 24 h. At 72 h, large number of cells in this zone had liquefied and lost their cellular structures (Figure 1D, 1F and 1H, left). The intermediate and outer zones of the MWA and RFA lesions degenerated quickly in the same manner. The major findings at 12 h included interstitial edema, cell rupture and nuclear loss. More severe tissue degradation was observed at 24 and 72 h (Figure 1, middle). At 12 h, the borderline between the ablated and intact liver was well established by H&E staining in both MWA and RFA samples (Figure

1C, 1D, right). Neutrophils, macrophages, and fibroblasts from the surrounding intact liver infiltrated the outer zones first and then to the intermediate zone (Figure 1E-H, middle and right).

AcP activity was altered in the outer zones of both MWA and RFA lesions. In the outer zone hepatocytes, AcP activity present immediately after ablation had disappeared at subsequent time points concomitantly with the presence of AcP activity in newly infiltrated cells. Consequently, a new pattern of positive AcP staining was observed beginning 24 h after ablation (Figure 2).

Comparison of MWA and RFA

Assessment of vessel and bile duct injuries, **Figure 3** shows the normal, immediately, 24, and 72 h after ablation hepatic portal triads (**Figure 3A-E**, respectively). Injuries of veins, arteries, and bile ducts occurred similarly following MWA and RFA. Vessel injuries consisted of loss of endothelium causing extravasation of red blood cells, deformation or loss of nuclei, acidophilic cytoplasm, and sloughed off endothelium (**Figure 3B-E**). Injuries of bile duct cells were less severe with blurred cell wall and normal or deformed cell nuclei. Structure of bile duct in the outer zones of ablated regions was preserved and no biloma was found in all samples (**Figure 3D, 3E**). Neighboring ablated region bile ducts were well maintained their structure and cell shape (**Figure 3F**). The hepatocytes surrounding portal triad were completely ablated in MWA samples whereas a number of non-ablated hepatocytes sometimes appeared on outer side of portal triad in RFA samples (**Figure 3C**). The phenomenon was thought as a consequence of heat sink effect. In this ablation model, the insufficiently ablated hepatocytes appeared beside vessels with diameter of 120 microns or larger and distance to the RFA needle of 3 mm or farther.

Observation at a low magnification (10×) revealed differences in the margins and shapes of the regions ablated using MWA and RFA. MWA induced a sharp demarcation between the ablated and non-ablated regions, whereas RFA induced an irregular ablated margin (**Figure 4A, 4C, 4E** vs **Figure 4B, 4D, 4F**, respectively). Intralesional cell survival was sometimes observed in the outer zone of RFA samples, especially perivascular regions (**Figure 4D**). The presence of blood vessels in or around this zone affected the shape of the ablated region. This effect led to greater irregularity in the shape of RFA lesions compared with MWA lesions.

Discussion

AcP staining is reportedly useful for cell death detection and early delineation of ablated regions, which are poorly defined by H&E staining, particularly following MWA [18-20]. In this study, MWA and RFA induced similar alterations in AcP activity in the ablated region at every time point tested. Therefore, AcP staining allowed delineation of the lesions immediately

after ablation, but did not reveal any differences between these two ablative techniques.

In addition, no differences between MWA and RFA in terms of macroscopic tissue changes and the ablation zone size were observed. However, differences in tissue changes were visible at a microscopic level. Tissue in RFA-induced region exhibited early damage and disruption, whereas a portion of tissue around the microwave antenna comprised structurally stable hepatocytes that resembled living cells until 3 day after ablation. Therefore, AcP staining is necessary for defining cell viability in the MWA central zone. Although the cells in central zones of MWA and RFA lesions underwent different remodeling processes, both were negative for AcP activity indicating no evidence of viability.

In RFA lesions, the burned edge was less sharply demarcated than that in MWA lesions, which were less affected by heat dissipation via blood vessels. These differences were potentially the result of the specific heating mechanisms used in each technique. Microwaves induce direct heating in a large volume of tissue around the antenna and the tissue within this volume is uniformly and consistently heated during microwave irradiation. This can propagate through tissue without depending on electric conductivity [4, 7, 17, 21]. Consequently, tissue within the direct heating region undergoes homogenous cellular desiccation and protein coagulation, a process known as microwave tissue fixation [11, 19]. In contrast, tissue heating is inconsistent and inhomogeneous in RFA because the resistive heating induced by the electric current is modulated by the local tissue impedance and current density. Impedance depends on the ionic concentration of the tissue, which is attenuated quickly during RFA because of water vaporization, and the current density is inversely proportional to the distance from the electrode. Furthermore, the tissue is primarily ablated by thermal conduction, which is strongly influenced by the heat-sink effect [4].

In 1990, both McGahan *et al.* and Rossi *et al.* independently published the first reports of RFA application for liver tumor ablation [22, 23]. Thereafter, this technique has been increasingly used worldwide. In 1994, MWA was introduced as a therapeutic modality for hepatocellular carcinoma [24]. Although MWA

Comparison of MWA and RFA

has been widely accepted during the past two decades, RFA currently remains the most popular method of liver tumor ablation [6]. Comparison of MWA and RFA in both animal and clinical studies have revealed the superiority of MWA over RFA in terms of larger ablated zones, better lesion demarcation, reduced heat-sink effect, no limitations from tissue charring, ability to exploit electromagnetic field overlap and thus enhance heating by applying a multiple-antenna array, and no requirement for a ground pad to prevent the risk of skin burns [1, 4, 7, 12-16]. The key issue associated with MWA is the effective transmission of microwave power to tissues. Developments in the field of MWA technology should focus on the designs of microwave antennae and generators to address the major problems associated with MWA such as microwave reflection, frequency drift, and reduced generator effectiveness [21, 25].

In conclusion, tissue changes associated with MWA included tissue fixation in the central zone under direct heating and thermal conduction with early tissue disruption in the outer zone. In addition, MWA was less influenced by heat-sink effect and could create a regularly shaped ablated lesion with a sharp burned edge. In contrast, the entire ablated region underwent a progressive damage process with RFA. The ablated lesion was irregularly shaped as a result of neighboring blood vessels and intralesional cell survival was sometimes evident in the outer zone. This comparison revealed differences in tissue responses to the resistive heating of RFA and magnetic field induction heating of MWA. These findings consolidate the advantages of microwave technology relative to radiofrequency. MWA should therefore be completely developed to obtain the more reliable and controllable ablation zones and should be the recommended technique option in future.

Disclosure of conflict of interest

None.

Address correspondence to: Dr. Nguyen Quoc Vinh, Department of Surgery, Shiga University of Medical Science, Seta-Tsukinowa, Otsu, Shiga 520-2192, Japan. Tel: +81-77-548-2238; Fax: +81-77-548-2240; E-mail: vinh@belle.shiga-med.ac.jp

References

- [1] Munireddy S, Katz S, Somasundar P and Espat NJ. Thermal tumor ablation therapy for colorectal cancer hepatic metastasis. *J Gastrointest Oncol* 2012; 3: 69-77.
- [2] Crocetti L and Lencioni R. Thermal ablation of hepatocellular carcinoma. *Cancer Imaging* 2008; 8: 19-26.
- [3] McDermott S and Gervais DA. Radiofrequency Ablation of Liver Tumors. *Semin Interv Radiol* 2013; 30: 49-55.
- [4] Brace CL. Radiofrequency and Microwave Ablation of the Liver, Lung, Kidney, and Bone: What Are the Differences? *Curr Probl Diagn Radiol* 2009; 38: 135-143.
- [5] Kim Y, Rhim H, Lim H, Choi D, Lee M and Park M. Coagulation Necrosis Induced by Radiofrequency Ablation in the Liver: Histopathologic and Radiologic Review of Usual to Extremely Rare Changes. *Radiographics* 2011; 31: 377-390.
- [6] Hong K and Georgiades C. Radiofrequency Ablation: Mechanism of Action and Devices. *J Vasc Interv Radiol* 2010; 21: S179-S186.
- [7] Simon CJ, Dupuy DE and Mayo-Smith WW. Microwave Ablation: Principles and Applications. *Radiographics* 2005; 25: S69-S83.
- [8] Lubner MG, Brace CL, Hinshaw JL and Lee FT Jr. Microwave Tumor Ablation: Mechanism of Action, Clinical Results, and Devices. *J Vasc Interv Radiol* 2010; 21: S192-S203.
- [9] Goldberg S, Gazelle G, Compton C, Mueller P and Tanabe K. Treatment of intrahepatic malignancy with radiofrequency ablation: radiologic-pathologic correlation. *Cancer* 2000; 88: 2452-2463.
- [10] Ohno T, Kawano K, Sasaki A, Aramaki M, Yoshida T and Kitano S. Expansion of an ablated site and induction of apoptosis after microwave coagulation therapy in rat liver. *J Hepatobiliary Pancreat Surg* 2001; 8: 360-366.
- [11] Ozaki T, Mori I, Nakamura M, Utsunomiya H, Tabuse K and Kakudo K. Microwave cell death: Immunohistochemical and enzyme histochemical evaluation. *Pathol Int* 2003; 53: 686-692.
- [12] Bhardwaj N, Strickland AD, Ahmad F, Atanesyan L, West K and Lloyd DM. A comparative histological evaluation of the ablations produced by microwave, cryotherapy and radiofrequency in the liver. *Pathology* 2009; 41: 168-172.
- [13] Fan W, Li X, Zhang L, Jiang H and Zhang J. Comparison of Microwave Ablation and Multipolar Radiofrequency Ablation In Vivo Using Two Internally Cooled Probes. *AJR Am J Roentgenol* 2012; 198: W46-W50.
- [14] Laeseke PF, Lee FT Jr, Sampson LA, van der Weide DW and Brace CL. Microwave Ablation versus Radiofrequency Ablation in the Kidney:

Comparison of MWA and RFA

- High-power Triaxial Antennas Create Larger Ablation Zones than Similarly Sized Internally Cooled Electrodes. *J Vasc Interv Radiol* 2009; 20: 1224-1229.
- [15] Wright A, Sampson L, Warner T, Mahvi D and Lee F. Radiofrequency versus Microwave Ablation in a Hepatic Porcine Model. *Radiology* 2005; 236: 132-139.
- [16] Zhang L, Wang N, Shen Q, Cheng W and Qian GJ. Therapeutic Efficacy of Percutaneous Radiofrequency Ablation versus Microwave Ablation for Hepatocellular Carcinoma. *PLoS One* 2013; 8: e76119.
- [17] Andreano A and Brace C. A Comparison of Direct Heating During Radiofrequency and Microwave Ablation in Ex Vivo Liver. *Cardiovasc Intervent Radiol* 2013; 36: 505-511.
- [18] Mukaisho K, Sugihara H, Tani T, Kurumi Y, Kamitani S, Tokugawa T and Hattori T. Effects of Microwave Irradiation on Rat Hepatic Tissue Evaluated by Enzyme Histochemistry for Acid Phosphatase. *Dig Dis Sci* 2002; 47: 376-379.
- [19] Yamaguchi T, Mukaisho K, Yamamoto H, Shiomi H, Kurumi Y, Sugihara H and Tani T. Disruption of Erythrocytes Distinguishes Fixed Cells/Tissues from Viable Cells/Tissues Following Microwave Coagulation Therapy. *Dig Dis Sci* 2005; 50: 1347-1355.
- [20] Mukaisho K, Kurumi Y, Sugihara H, Naka S, Kamitani S, Tsubosa Y, Moritani S, Endo Y, Hanasawa K, Morikawa S, Inubushi T, Hattori T and Tani T. CASE REPORT: Enzyme Histochemistry Is Useful to Assess Viability of Tumor Tissue After Microwave Coagulation Therapy (MCT): Metastatic Adenocarcinoma Treated by Lateral Segmentectomy After MCT. *Dig Dis Sci* 2002; 47: 2441-2445.
- [21] Tabuse K. Basic knowledge of a microwave tissue coagulator and its clinical applications. *Jo Hepatobiliary Pancreat Surgery* 1998; 5: 165-172.
- [22] McGahan J, Browning P, Brock J and Tesluk H. Hepatic ablation using radiofrequency electrocautery. *Invest Radiol* 1990; 25: 267-270.
- [23] Rossi S, Fornari F, Pathies C and Buscarini L. Thermal lesions induced by 480 KHz localized current field in guinea pig and pig liver. *Tumori* 1990; 76: 54-57.
- [24] Seki T, Wakabayashi M, Nakagawa T, Itho T, Shiro T, Kunieda K, Sato M, Uchiyama S and Inoue K. Ultrasonically guided percutaneous microwave coagulation therapy for small hepatocellular carcinoma. *Cancer* 1994; 74: 817-825.
- [25] Brace CL. Microwave Tissue Ablation: Biophysics, Technology and Applications. *Crit Rev Biomed Eng* 2010; 38: 65-78.